PROTEINS
STRUCTURE ■ FUNCTION ■ BIOINFORMATICS

Effectiveness and limitations of local structural entropy optimization in the thermal stabilization of mesophilic and thermophilic adenylate kinases

Sojin Moon,[1] Ryan M. Bannen,[2] Thomas J. Rutkoski,[3] George N. Phillips Jr.,[2,3,4] and Euiyoung Bae[1,5,6]*

[1] Department of Agricultural Biotechnology, Seoul National University, Seoul 151-921, Korea
[2] Department of Biochemistry, University of Wisconsin-Madison, Madison, WI 53706
[3] Center for Eukaryotic Structural Genomics, University of Wisconsin-Madison, Madison, WI 53706
[4] Department of Biochemistry and Cell biology, Rice University, Houston, TX 77005
[5] Center for Food and Bioconvergence, Seoul National University, Seoul 151-921, Korea
[6] Research Institute of Agriculture and Life Sciences, Seoul National University, Seoul 151-921, Korea

ABSTRACT

Local structural entropy (LSE) is a descriptor for the extent of conformational heterogeneity in short protein sequences that is computed from structural information derived from the Protein Data Bank. Reducing the LSE of a protein sequence by introducing amino acid mutations can result in fewer conformational states and thus a more stable structure, indicating that LSE optimization can be used as a protein stabilization method. Here, we describe a series of LSE optimization experiments designed to stabilize mesophilic and thermophilic adenylate kinases (AKs) and report crystal structures of LSE-optimized AK variants. In the mesophilic AK, thermal stabilization by LSE reduction was effective but limited. Structural analyses of the LSE-optimized mesophilic AK variants revealed a strong correlation between LSE and the apolar buried surface area. Additional mutations designed to introduce noncovalent interactions between distant regions of the polypeptide resulted in further stabilization. Unexpectedly, optimizing the LSE of the thermophilic AK resulted in a decrease in thermal stability. This destabilization was reduced when charged residues were excluded from the possible substitutions during LSE optimization. These observations suggest that stabilization by LSE reduction may result from the optimization of local hydrophobic contacts. The limitations of this process are likely due to ignorance of other interactions that bridge distant regions in a given amino acid sequence. Our results illustrate the effectiveness and limitations of LSE optimization as a protein stabilization strategy and highlight the importance and complementarity of local conformational stability and global interactions in protein thermal stability.

Proteins 2014; 82:2631–2642.

Key words: protein stability; thermal stability; structural biology; protein engineering; biotechnology.

INTRODUCTION

Proteins that are stable at high temperatures are favored in many industrial and laboratory applications.[1–7] Thermally stable proteins allow for high reaction temperatures facilitating accelerated reaction rates, increased solubility of reactants and products, and reduced microbial contamination. Thermal stability is also important for developing robust enzymes for use in industrial processes and for manufacturing protein-based pharmaceuticals with improved efficacy and longer shelf lives. In a

Additional Supporting Information may be found in the online version of this article.
Ryan M. Bannen's current address is Roche NimbleGen, Madison, WI 53719.
Grant sponsor: Basic Science Research Program, National Research Foundation of Korea (NRF), Ministry of Education, Science and Technology; grant number: 2009-0067791; Grant sponsor: Cooperative Research Program for Agricultural Science and Technology Development, Rural Development Administration; grant number: PJ009781.
*Correspondence to: Euiyoung Bae, Department of Agricultural Biotechnology, Seoul National University, Seoul 151-921, Korea. E-mail: bae@snu.ac.kr
Received 13 May 2014; Revised 9 June 2014; Accepted 9 June 2014
Published online 13 June 2014 in Wiley Online Library (wileyonlinelibrary.com).
DOI: 10.1002/prot.24627

laboratory setting, stable proteins are more convenient to store and handle and are often required in experimental protocols such as polymerase chain reactions.

A number of experimental and computational approaches have been developed to redesign proteins to become more thermally stable. One approach is structure-based rational design, which involves specific, structure-guided mutagenesis for increasing conformational stability.[5,7–10] The mutations are designed to introduce stabilizing structural elements such as ion pairs, hydrogen bonds, and hydrophobic interactions. Despite numerous successes, this approach has several limitations as a protein stabilization method. Detailed structural information on the target protein, such as a high-resolution crystal structure, must be available. Another limitation is the lack of a general protocol for determining the positions and types of mutations to be introduced. Therefore, this approach is essentially target-specific and difficult to automate.

Experimental evolution can also be used to enhance protein thermal stability.[11–14] In this nonrational approach, a target protein is randomly mutated in a laboratory and evaluated for a desired trait such as, in this case, increased thermal stability. This method does not require *a priori* knowledge of the target protein's three-dimensional structure but may require extensive experimentation and substantial laboratory resources. Thus, experimental evolution can be time-consuming and expensive.

Another approach for improving protein thermal stability is the consensus method, which aims to find commonality in the sequences of proteins within a family.[15–17] In this computational approach, a sequence alignment is performed using a target and many homologous proteins to identify conserved and/or major amino acids in particular positions. This technique is based on the assumption that these "consensus" amino acids are crucial for maintaining the structure shared by homologous proteins and therefore contribute more significantly to stability than do nonconsensus amino acids. Although detailed structural information or substantial experimental efforts may not be necessary, the consensus approach requires a large number of homologous sequences and often arbitrary constraints when the sequence alignments do not clearly indicate dominant amino acids at given positions.

We previously developed a bioinformatic approach for designing more stable proteins based on measures of local structural entropy (LSE).[18] The concept of LSE was first developed by Hwang and coworkers[19] to describe the extent of conformational heterogeneity in short protein sequences. By carefully examining structures deposited in the Protein Data Bank,[20] they calculated the LSE of certain amino acid tetramers and compiled a database of 4^{20} possible tetramer sequences. In this process, tetramers that appeared in various secondary structures were assigned higher LSE values than those always adopting a single secondary structural element. They also found that differences in the average LSE of thermophilic proteins and their mesophilic homologues correlated with their respective differences in thermal stability.[19]

In our previous study, LSE was incorporated as part of a protein stabilization method applied to adenylate kinase (AK) from a mesophilic bacterium, *Bacillus subtilis* (AKmeso).[18] The average LSE of AKmeso was reduced by substituting amino acid residues with those from a homologous protein from a psychrophilic bacterium, *Bacillus globisporus* (AKpsychro). Despite using a less thermally stable homologue for these residue substitutions, three of the LSE-optimized variant proteins (AKlse1, AKlse2, and AKlse3) exhibited considerably higher thermal denaturation midpoint (T_m) than that of AKmeso. More recently, we demonstrated that the extent of thermal stabilization by LSE optimization was comparable with that obtained using other approaches[21] including structure-guided mutagenesis[22,23] and experimental evolution.[24] That study also reported the crystal structure of an LSE-optimized AKmeso variant, AKlse1. However, the structure failed to reveal any clear structural mechanisms that could account for the observed increase in thermal stability.[21]

In this study, we designed additional LSE-optimized AK variants and evaluated their thermal stabilities to expand our understanding of LSE in protein stability and its use for thermal stabilization. The LSE of AKmeso was reduced further in an attempt to achieve more substantial stabilization, and the effects of LSE optimization were also tested with AK from a thermophilic bacterium, *Geobacillus stearothermophilus* (AKthermo). Crystal structures of LSE-optimized AK variants were solved to identify the structural bases of thermal stabilization by LSE optimization. Our results illustrate the effectiveness and the limitations of LSE optimization as a thermal stabilization approach in proteins.

MATERIALS AND METHODS

Generation of LSE-optimized AK variants

Sequences of LSE-optimized AK variants were generated as described previously.[18,25] The genes encoding the variants were prepared commercially or by polymerase chain reactions using mismatched primers in pET11a vectors. The proteins were overexpressed in *Escherichia coli* and purified by a two-step procedure involving affinity chromatography using Affi-Gel blue resin (Bio-Rad, Hercules, CA) and size exclusion chromatography as described previously.[22]

Determination of T_m values

T_m values of the LSE-optimized AK variants were determined by circular dichroism (CD) spectroscopy as described previously.[21] Briefly, CD traces of the AK variants were measured at 220 nm at a scanning rate of

1°C/min. CD data were analyzed based on the protocol developed by John and Weeks[26] using Kaleidagraph (Synergy Software).

Crystallization

AKlse2 crystals were grown at 20°C by the hanging-drop method from 10 mg/mL protein and 4 m*M* P^1,P^5-di(adenosine 5′)-pentaphosphate (Ap_5A) in buffer (10 m*M* HEPES pH 7.0) mixed with an equal amount of reservoir solution (1.9 *M* ammonium citrate pH 6.0). The crystals were cryoprotected in the reservoir solution supplemented with 30% (v/v) glycerol and flash-frozen in liquid nitrogen.

AKlse3 crystals were grown at 20°C by the hanging-drop method from 15 mg/mL protein and 4 m*M* Ap_5A in buffer (10 m*M* HEPES pH 7.4) mixed with an equal amount of reservoir solution (29% (w/v) polyethylene glycol monomethyl ether 2000, 100 m*M* $CaCl_2$, 100 m*M* 3-[4-(2-hydroxyethyl)-1-piperazinyl]propanesulfonic acid pH 8.0). The crystals were flash-frozen in liquid nitrogen without additional cryoprotecting reagents.

AKlse4 crystals were grown at 20°C by the hanging-drop method from 30 mg/mL protein and 4 m*M* Ap_5A in buffer (10 m*M* HEPES pH 7.0) mixed with an equal amount of reservoir solution (32% (w/v) polyethylene glycol 4000, 250 m*M* $MgCl_2$, 100 m*M* Tris pH 8.5). The crystals were cryoprotected in the reservoir solution supplemented with 20% (v/v) glycerol and flash-frozen in liquid nitrogen.

AKlse5 crystals were grown at 20°C by the hanging-drop method from 10 mg/mL protein and 4 m*M* Ap_5A in buffer (10 m*M* HEPES pH 7.0) mixed with an equal amount of reservoir solution (26.5% (w/v) polyethylene glycol 4000, 150 m*M* magnesium acetate, 100 m*M* sodium cacodylate pH 6.5). The crystals were cryoprotected in the reservoir solution supplemented with 10% (v/v) glycerol and flash-frozen in liquid nitrogen.

AKlse6 crystals were grown at 20°C by the hanging-drop method from 13 mg/mL protein and 4 m*M* Ap_5A in buffer (10 m*M* HEPES pH 7.0) at the same conditions as those used for obtaining AKlse5 crystals. The crystals were cryoprotected in the reservoir solution supplemented with 10% (v/v) glycerol and flash-frozen in liquid nitrogen.

Structure determination

Diffraction data of AKlse2, AKlse4, AKlse5, and AKlse6 were collected at 100 K at the beamline 7A of the Pohang Accelerator Laboratory. The GM/CA-CAT beamline of the Advanced Photon Source was used to obtain diffraction data of AKlse3. Diffraction images were processed with HKL2000.[27] Phaser[28] was used for molecular replacement phasing for all crystals except AKlse3, which was solved using MOLREP.[29] The structure of AKlse1 was used as a starting model for AKlse2, AKlse3, and AKlse4. Solutions for AKlse5 and AKlse6 were found using the structure of AKthermo. The final structures were completed using alternate cycles of manual fitting in COOT[30] and refinement in REFMAC5.[31] The stereochemical quality of the final models was assessed using MolProbity.[32]

Structural analysis

The five C-terminal residues (residues 213–217) were not included in structural analyses because they were not resolved in the AKmeso structure. Protein Data Bank codes for the structures of AKmeso,[22] AKthermo,[33] and AKlse1[21] used in the analyses were 1P3J, 1ZIO, and 4MKG, respectively. Two oppositely charged residues were identified as an ion pair if their closest charged atoms were within 4 Å. The side-chain oxygen atoms of Asp and Glu were considered negatively charged atoms and the side-chain nitrogen atoms of Arg and Lys were considered positively charged atoms. Hydrogen bonds were identified using WHAT IF.[34] Accessible and buried molecular surface areas were calculated with WHAT IF using a probe radius of 1.4 Å.[34] Nitrogen and oxygen atoms were considered polar. Carbon and sulfur atoms were considered apolar.

Accession numbers

The atomic coordinates and structure factors of AKlse2 to AKlse6 were deposited in the Protein Data Bank with the accession codes 4QBF, 3DL0, 4QBG, 4QBH, and 4QBI, respectively.

RESULTS

Thermal stabilization by LSE optimization was effective but limited in mesophilic AK

The LSE optimization of AKmeso was performed previously by substituting several of its amino acid residues with those from AKpsychro, resulting in three LSE-optimized AK variants (Fig. 1; Table I).[18] Only residues in the CORE domain (residues 1–30, 61–126, and 165–217) were substituted because this central domain almost exclusively controls the overall stability of AK.[35] This process can result in a total of 2^{53} variant sequences because the mesophilic and psychrophilic AKs differ by 53 residues in the CORE domain (Fig. 1). Among these variants, AKlse1, with 23 substitutions, was optimal. AKlse2 was only slightly less optimized than AKlse1, but contained the largest number (26) of residue substitutions of the top 20 LSE-optimized AK variants. AKlse3 was considerably less LSE-optimized than AKlse1 and AKlse2 and contained only 10 substitutions. AKlse3 was designed to avoid any "AKthermo-like" substitutions, in which the resulting amino acids would be identical to

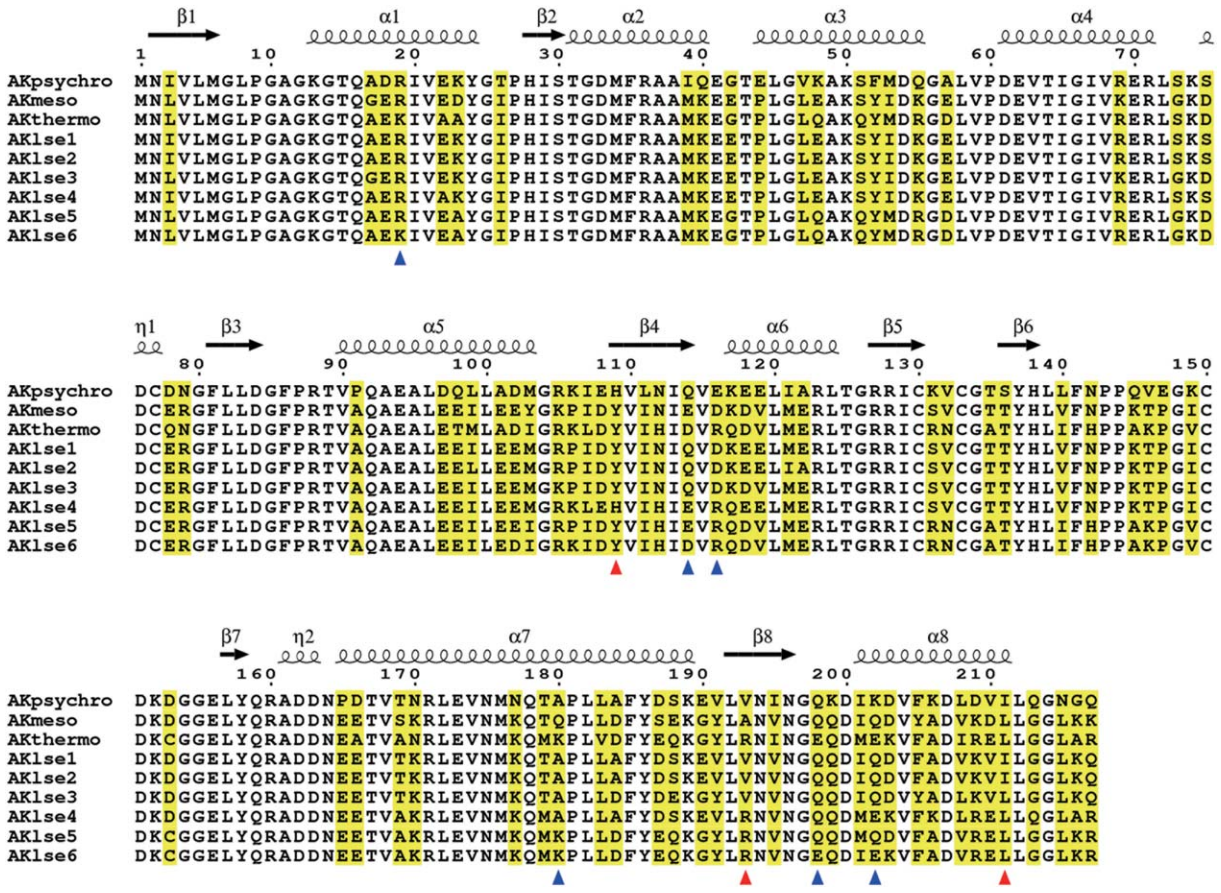

Figure 1

Sequence alignment of WT AKs and LSE-optimized AK variants. The amino acid sequences of three WT AKs (AKpsychro, AKmeso, and AKthermo) and six LSE-optimized AK variants (AKlse1 to AKlse6) are aligned together. Variable residues are highlighted, and secondary structure elements are represented based on the structure of AKmeso. The positions of the three AKthermo ion pairs (Lys19-Glu202, Arg116-Glu198, and Lys180-Asp114) are marked with blue triangles. The positions of the three residues (Tyr109, Val193, and Ile211) making hydrophobic contact in AKlse1 are indicated by red triangles. [Color figure can be viewed in the online issue, which is available at wileyonlinelibrary.com.]

those in AKthermo, although the substitutions were originally chosen based on comparison with AKpsychro.

Another LSE-optimized variant, AKlse4, was designed using AKmeso as a template (Fig. 1; Table I). To more significantly reduce the LSE of AKmeso, residue substitutions were allowed from both AKpsychro and AKthermo. This resulted in a much larger search space ($2^{44}\cdot3^{19}$ vs. 2^{53}) in which to identify an optimal sequence. AKmeso contains a total of 63 residues in the CORE domain that differ from those of either AKpsychro or AKthermo, including 19 positions where amino acids are different in all three of the wild-type (WT) AKs (Fig. 1). Consequently, AKlse4, the most LSE-optimized variant generated in this process, contains more residue substitutions and a lower average LSE value than those of the three previously designed variants (Table I).

Thermal stabilization was evaluated experimentally for AKlse2, AKlse3 and AKlse4 using CD spectroscopy (Supporting Information Fig. S1). Previously reported T_m values for AKlse2 and AKlse3 were determined using differential scanning calorimetry (DSC),[18] and T_m values can vary substantially depending on the experimental techniques and procedures by which they are measured. CD data of AKmeso and AKlse1 are available from our previous study.[21] T_m values of the four LSE-optimized AK variants (AKlse1 to AKlse4) and their template, AKmeso, which were obtained using the same instrumentation and experimental conditions, are listed in Table I.

As expected, AKlse2 and AKlse3 were more thermally stable than AKmeso, with T_m values 9.8°C and 3.7°C greater than that of AKmeso, respectively. The T_m increases measured previously using DSC were 12.5°C and 5.0°C, respectively.[18] A strong correlation was observed between the three previously designed LSE-optimized AK variants and AKmeso, as indicated by a plot of T_m as a function of average LSE [Fig. 2(A)]. While AKlse4 exhibited a higher T_m value than AKmeso,

Table I
Design Strategy and Properties of LSE-Optimized AK Variants

	Template	Substitutions from	Additional design constraint/strategy	Number of substitutions	Average LSE[a]	T_m (°C)	ΔT_m (°C)[b]
AKmeso	N/A	N/A	N/A	N/A	1.4938	46.4[c]	N/A
AKlse1[d]	AKmeso	AKpsychro	None	23	1.4083	57.7[c]	11.3
AKlse2[d]	AKmeso	AKpsychro	The most substitutions in the top 20 most optimized variants	26	1.4085	56.2	9.8
AKlse3[d]	AKmeso	AKpsychro	No "AKthermo-like" substitutions	10	1.4603	50.1	3.7
AKlse4	AKmeso	AKpsychro, AKthermo	None	38	1.3696	56.6	10.2
AKlse4m1	AKmeso	AKpsychro, AKthermo	Three ion pairs[e] from AKthermo added on AKlse4	41	1.3808	58.4	12.0
AKlse4m2	AKmeso	AKpsychro, AKthermo	Hydrophobic contact[f] from AKlse1 added on AKlse4	38	1.3773	58.2	11.8
AKthermo	N/A	N/A	N/A	N/A	1.4323	74.5[g]	N/A
AKlse5	AKthermo	AKmeso	None	21	1.3905	65.1	−9.4
AKlse6	AKthermo	AKmeso	Charged residues excluded for substitutions	15	1.4068	70.7	−4.5

[a]Calculated for CORE domain (residues 1–30, 61–126, and 165–212) using the program downloaded from http://sdse.life.nctu.edu.tw (Ref. 19).
[b]Difference from T_m of the respective template AKs.
[c]From Ref. 21.
[d]Designed previously in Ref. 18.
[e]Lys19-Glu202, Arg116-Glu198, and Lys180-Asp114.
[f]Tyr109, Val193, and Ile211.
[g]From Ref. 36.

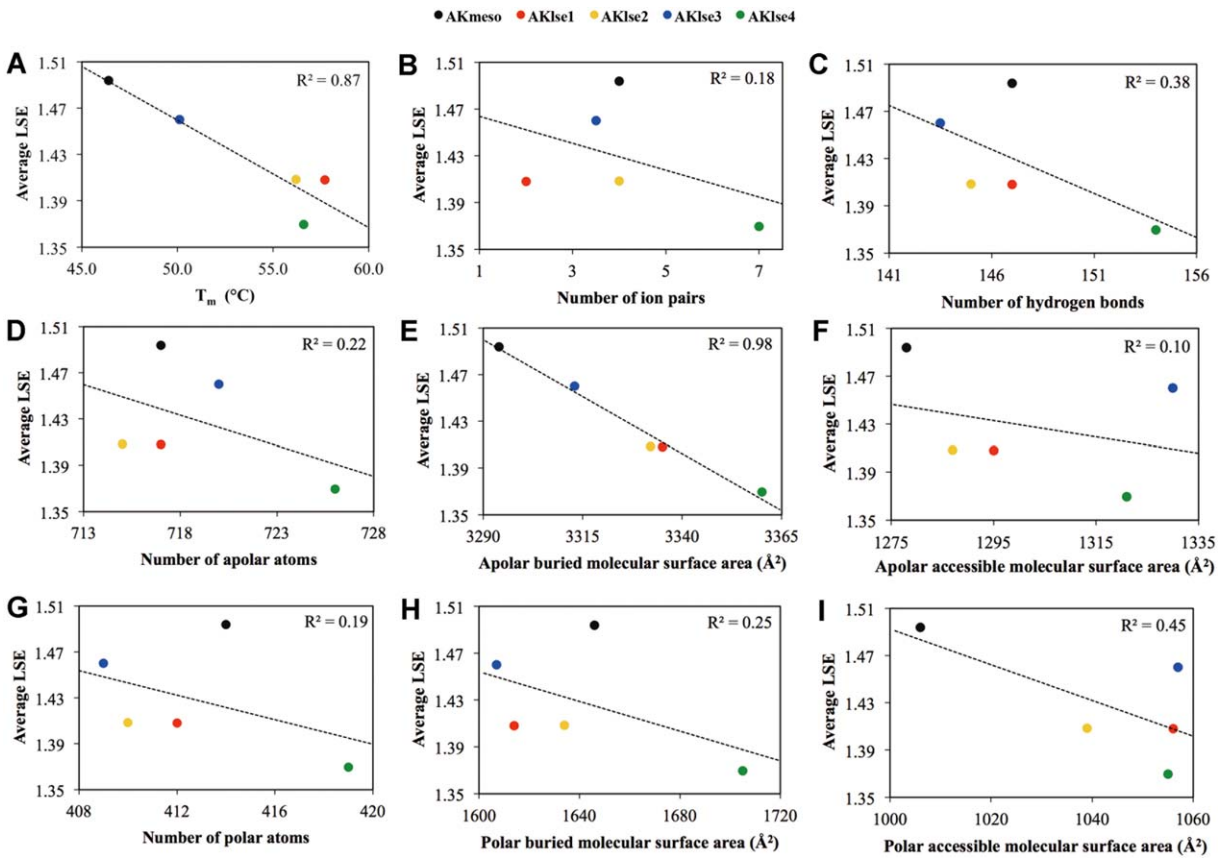

Figure 2
Correlations between LSE and structural features in four LSE-optimized AKmeso variants (AKlse1 to AKlse4) and their template, AKmeso. Data for the five AKs are represented by different colors (AKmeso: black; AKlse1: red; AKlse2: yellow; AKlse3: blue; AKlse4: green). Trend lines and R^2 values are also shown.

Table II
Data Collection and Refinement Statistics for Structures of LSE-Optimized AK Variants[a]

	AKlse2	AKlse3	AKlse4	AKlse5	AKlse6
Space group	$P2_12_12_1$	$P2_1$	C2	$P2_1$	$P2_1$
Unit cell parameters (Å)	$a = 39.3$, $b = 47.2$, $c = 109.3$	$a = 34.0$, $b = 76.7$, $c = 78.0$, $\beta = 95.3°$	$a = 68.8$, $b = 71.0$, $c = 45.6$, $\beta = 95.1°$	$a = 36.1$, $b = 75.4$, $c = 82.0$, $\beta = 90.0°$	$a = 36.8$, $b = 76.5$, $c = 85.1$, $\beta = 90.2°$
Wavelength (Å)	0.9795	0.9793	0.9795	0.9793	0.9793
Data collection statistics					
Resolution range (Å)	50.00–1.80 (1.86–1.80)	50.00–1.53 (1.58–1.53)	50.00–1.37 (1.42–1.37)	50.00–1.68 (1.74–1.68)	50.00–1.67 (1.73–1.67)
Number of reflections (measured/unique)	135,728/19418	216,791/594,16	165,077/442,20	358,723/494,58	202,169/548,22
Completeness (%)	99.9 (100.0)	98.9 (91.1)	97.0 (95.1)	97.6 (95.7)	100.0 (100.0)
R_{merge}[b]	0.107 (0.752)	0.067 (0.406)	0.047 (0.720)	0.074 (0.728)	0.094 (0.617)
Redundancy	7.0 (7.1)	3.6 (2.3)	3.7 (3.6)	7.3 (7.1)	3.7 (3.7)
Mean I/σ	15.6 (4.0)	16.5 (2.4)	14.5 (2.4)	22.8 (2.7)	12.8 (2.2)
Refinement statistics					
Resolution range (Å)	50.00–1.80	50.00–1.58	49.32–1.37	50.00–1.68	50.00–1.67
R_{cryst}[c]/R_{free}[d] (%)	17.1/22.2	20.2/23.9	17.9/22.0	17.8/22.4	16.8/20.8
RMSD bonds (Å)	0.019	0.012	0.026	0.020	0.025
RMSD angles (°)	2.332	1.508	2.510	2.186	2.428
Average B factor (Å^2)	20.02	18.39	17.91	18.59	22.04
Number of water molecules	144	535	232	401	537
Ramachandran favored (%)	99.1	99.3	100.0	98.8	98.4
Ramachandran allowed (%)	0.9	0.7	0.0	1.2	1.6

[a]Values in parentheses are for the highest-resolution shell.
[b]$R_{merge} = \Sigma_h\Sigma|I_i(h) - <I(h)>|/\Sigma_h\Sigma_iI_i(h)$, where $I_i(h)$ is the intensity of an individual measurement of the reflection and $<I(h)>$ is the mean intensity of the reflection.
[c]$R_{cryst} = \Sigma_h||F_{obs}| - |F_{calc}||/\Sigma_h|F_{obs}|$, where F_{obs} and F_{calc} are the observed and calculated structure factor amplitudes, respectively.
[d]R_{free} was calculated as R_{cryst} using 5% of the randomly selected unique reflections that were omitted from structure refinement.

the extent of stabilization was not as significant as expected based on its LSE value (Table I). Despite its considerably lower LSE value, which implies greater thermal stabilization, AKlse4 exhibited a smaller T_m increase (10.2°C) than AKlse1 (11.3°C), weakening the overall correlation. As its LSE was reduced, the thermal stability of AKmeso seemed to increase only to a certain degree, suggesting that thermal stabilization by LSE optimization is limited.

Structural analysis revealed a strong correlation between LSE and apolar buried surface area

The crystal structure of AKlse1 was previously compared with that of AKmeso, but no clear structural mechanism was identified that could account for the increased thermal stability of AKlse1.[21] This study provides crystal structures of three additional LSE-optimized AK variants (AKlse2, AKlse3, and AKlse4). Data collection and refinement statistics are summarized in Table II. The asymmetric unit of AKlse3 contains two chains while only one chain was found in the structures of AKlse2 and AKlse4. The three variants were crystallized with the inhibitor Ap_5A in their active sites, as were AKmeso and AKlse1. The chain folds of the four variants and AKmeso are essentially identical (Supporting Information Fig. S2). The root mean square deviation (RMSD) values of Cα atom positions between AKmeso and each of the four LSE-optimized variants range from 0.6 to 2.1 Å.

To determine the molecular origins of the different thermal stabilities of the four LSE-optimized variants and their template, AKmeso, their crystal structures were compared with focus on the CORE domain where residue substitutions for LSE optimization were allowed. In our previous study, the mutations in the other two domains, AMP_{bind} and LID, did not result in considerable changes in the overall thermal stability of the enzyme.[35] Several structural features of their CORE domains were calculated and are listed in Table III, including the number of ion pairs, the number of hydrogen bonds, and the buried and accessible molecular surface areas.

Among the five AKs, AKlse4, whose LSE was reduced to the largest extent, contains the most ion pairs and hydrogen bonds. This variant also has the highest apolar buried surface area, which is often used as a measure of the degree of hydrophobic interactions. However, such stabilizing features were not always the least in AKmeso, which has the highest LSE value and was used as a template for generating the LSE-optimized variants. For example, AKmeso did not have the fewest ion pairs or hydrogen bonds. In fact, the numbers of ion pairs and

Table III
Structural Features of LSE-Optimized AK Variants[a]

	AKmeso	AKlse1	AKlse2	AKlse3[b]	AKlse4	AKthermo	AKlse5[b]	AKlse6[b]
Average LSE	1.4938	1.4083	1.4085	1.4603	1.3696	1.4323	1.3905	1.4068
T_m (°C)	46.4[c]	57.7[c]	56.2	50.1	56.6	74.5[d]	65.1	70.7
Number of ion pairs[e]	4 (2)	2 (0)	4 (2)	3.5 (1)	7 (1)	6 (3)	4 (2)	8 (3)
Number of hydrogen bonds[e]	147 (41)	147 (36)	145 (38)	143.5 (36.5)	154 (39)	157 (43)	141.5 (37.5)	148 (39)
Number of apolar atoms	717	717	715	720	726	718	726	727
Apolar buried molecular surface area (Å^2)	3294	3335	3332	3313	3360	3420	3338	3340
Apolar accessible molecular surface area (Å^2)	1278	1295	1287	1330	1321	1238	1305	1371
Number of polar atoms	414	412	410	409	419	411	419	417
Polar buried molecular surface area (Å^2)	1646	1614	1634	1607	1705	1675	1633	1670
Polar accessible molecular surface area (Å^2)	1006	1056	1039	1057	1055	1015	1117	1109

[a]Calculated for CORE domain (residues 1–30, 61–126, and 165–212).
[b]Average of the two chains in asymmetric unit.
[c]From Ref. 21.
[d]From Ref. 36.
[e]Values in parentheses are for interactions connecting distant regions (more than 10 residues in a polypeptide).

hydrogen bonds found in AKmeso are greater than or equal to those identified in the other three LSE-optimized variants (AKlse1, AKlse2, and AKlse3).

To identify the structural basis of thermal stabilization by LSE optimization more precisely, several plots were generated that describe the correlations between LSE and the structural features calculated based on the five structures (Fig. 2). Although the most LSE-optimized variant, AKlse4, revealed the most ion pairs and hydrogen bonds among the five AKs, correlations between the LSE and the numbers of ion pairs and hydrogen bonds were relatively weak [Fig. 2(B,C)]. Conversely, a strong correlation was observed between the average LSE and the apolar buried molecular surface area [Fig. 2(E)] This indicates that more apolar surface area becomes buried as the LSE is optimized. However, this is not entirely due to an increase in the number of apolar atoms upon LSE reduction because the correlation between the number of apolar atoms and LSE is poor ($R^2 = 0.22$) while the apolar buried surface area is almost perfectly correlated ($R^2 = 0.98$) with the average LSE value [Fig. 2(D,E)]. No such strong correlation with LSE was observed with other structural features (Fig. 2). These data suggest that LSE reduction may be closely related to the burial of apolar surface area, and that thermal stabilization via LSE optimization is a result of optimizing hydrophobic interactions.

LSE optimization overlooks and can damage stabilizing noncovalent interactions that connect distant regions of a polypeptide

Although AKlse4 was designed to have the lowest LSE value among the four LSE-optimized AKmeso variants (Table I), its T_m value was experimentally determined as 1.1°C lower than that of AKlse1, and only slightly higher (0.4°C) than that of AKlse2. This seems to indicate that an upper limit exists for the thermal stabilization of AKmeso by LSE optimization. The results of structural comparisons was also perplexing because the structure of AKlse4 appears to contain more stabilizing structural features, such as ion pairs, hydrogen bonds, and apolar buried surface area, than the other LSE-optimized AKmeso variants (Table III).

Because LSE describes conformational heterogeneity only in short stretches of a protein sequence, mutations designed to optimize LSE may disrupt noncovalent interactions that connect distant regions of a polypeptide. Such connections may be important for the overall stability of AKs.[21–23] Therefore, additional structural analyses were performed, focusing on stabilizing structural features that involve residues that are distant in sequence but adjacent in three-dimensional space. When considering the interactions between two amino acid residues separated by more than 10 residues in a single polypeptide, AKlse4 is no longer the variant with the most ion pairs and hydrogen bonds (see the values in parentheses in Table III). According to this definition for identifying interactions that work to connect distant regions, AKlse4 contains only one ion pair and 39 hydrogen bonds, both of which are fewer than those found in its template, AKmeso.

Three such ion pairs (Lys19-Glu202, Arg116-Glu198, and Lys180-Asp114) were found in the CORE domain of AKthermo[22] but were not introduced into AKlse4 [Fig. 3(A,B)], although residue substitutions were allowed from the thermophilic AK in the design of the AKlse4 sequence. This was because introducing AKthermo residues comprising these three ion pairs would result in unfavorable changes in LSE. In AKlse4, the three ion pairs of AKthermo are lost by residue mutations to uncharged amino acids or due to distances greater than the cutoff (4 Å) between the two oppositely charged residues.

A comparison of LSE-optimized AK variant structures also revealed an example in which hydrophobic interactions between distant regions in a given protein sequence

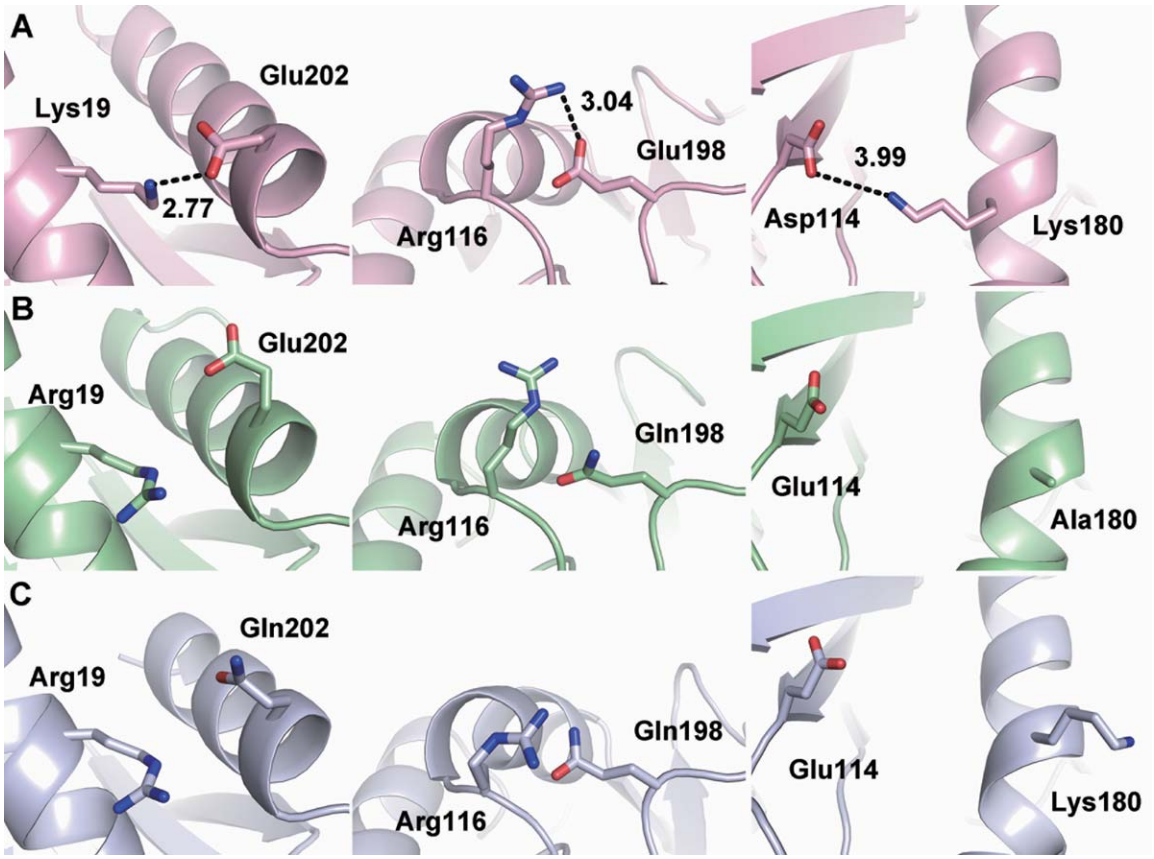

Figure 3

Loss of ion pairs during LSE optimization. In (**A**) AKthermo, three ion pairs (Lys19-Glu202, Arg116-Glu198, and Lys180-Asp114) connect distant regions of a polypeptide, but are lost by LSE optimization in (**B**) AKlse4 and (**C**) AKlse5. [Color figure can be viewed in the online issue, which is available at wileyonlinelibrary.com.]

were weakened due to residue substitutions designed to lower the LSE. In AKlse1 and AKlse2, Tyr109, Val193, and Ile211 make tight hydrophobic contacts within 4 Å, but are mutated to His, Arg, and Leu residues, respectively, in AKlse4 (Fig. 4). These LSE-reducing mutations disrupt the hydrophobic packing around the residues and decrease the apolar buried surface area (Table IV). Thus, our hypothesis is that the observed limit of LSE optimization on the thermal stabilization of AKmeso may result from ignorance with regard to the stabilizing effect of noncovalent interactions between distant regions of a polypeptide.

To experimentally validate this hypothesis, two mutants of AKlse4 were designed in which the lost noncovalent interactions were recovered. Then, the thermal stabilities of these mutants were measured to determine whether these interactions confer additional thermal stabilization (Table I). In the first AKlse4 mutant, AKlse4m1, the three AKthermo ion pairs (Lys19-Glu202, Arg116-Glu198, and Lys180-Asp114) were introduced. In AKlse4m2, the His109, Arg193, and Leu211 of AKlse4 were mutated to Tyr, Val, and Ile residues, respectively, to restore the hydrophobic interactions found in AKlse1 and AKlse2. In the measurements made with CD spectroscopy (Supporting Information Fig. S1), the two AKlse4 mutants displayed higher T_m values than that of AKlse4 (Table I). These results suggest that LSE reduction for the optimization of local structural properties overlooks and can potentially damage stabilizing, noncovalent interactions that bridge distant regions of a protein sequence.

LSE optimization of thermophilic AK resulted in decreased thermal stability

Although the four LSE-optimized AK variants and the two AKlse4 mutants exhibited considerable increases in their thermal stabilities compared with their template, AKmeso, none of them was more thermally stable than AKthermo, a naturally evolved thermophilic homologue of AKmeso. Despite high sequence identity (74.5%), AKmeso and AKthermo display disparate thermal stabilities.[22,36] The difference between their T_m values is more than 25°C.

In an attempt to produce a more stable AK variant than the natural thermophilic homologue, we designed an LSE-optimized AK variant using AKthermo as a

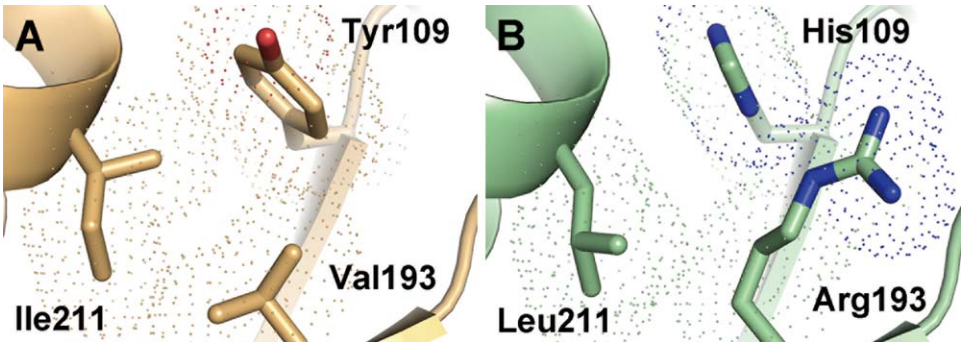

Figure 4

Effect of LSE-optimizing mutations on hydrophobic interactions. Tyr109, Val193, and Ile211 make tight hydrophobic contacts in (**A**) AKlse1, but are mutated to His, Arg, and Leu, respectively, in (**B**) AKlse4, disrupting the hydrophobic packing around the residues. For side-chain atoms of the three residues, van der Waals surfaces are represented. [Color figure can be viewed in the online issue, which is available at wileyonlinelibrary.com.]

template and residue substitutions allowed from AKmeso. The resulting lowest-LSE variant, AKlse5, contained 21 substituted residues in the CORE domain (Fig. 1; Table I). CD spectroscopy was used to measure the thermal stability of AKlse5 (Supporting Information Fig. S1). Surprisingly, the thermal stability of AKlse5 was not improved relative to its template, AKthermo, but rather exhibited a substantial decrease (9.4°C) in T_m despite a significantly lower LSE (Table I).

Based on the analysis of the LSE optimization of AKmeso, we suspected that this unexpected decrease in thermal stability of AKlse5 might be the result of damage to important, noncovalent stabilizing interactions between distant regions. One way to circumvent this problem would be to exclude residues involved in such interactions from LSE-optimizing substitutions. To test this possibility, another LSE-optimized AKthermo variant, AKlse6, was generated in which all formally charged residues (Arg, Lys, Asp, and Glu) were excluded from substitutions. As a result, AKlse6 contained a higher LSE value and fewer residue substitutions than did AKlse5 (Fig. 1; Table I). In the design of AKlse6, we intended to maintain bridging ion pairs by leaving out charged residues while optimizing the burial of apolar surface area, However, the T_m value of AKlse6 remained lower than that of AKthermo, although the extent of destabilization was reduced compared with AKlse5 (Table I).

Table IV

Effect of LSE Optimizing Residue Substitutions on Apolar Buried Surface Area of Residues 109, 193, and 211

	Apolar buried surface area (Å^2)						
	Residue 109		Residue 193		Residue 211		Total
AKlse1	Tyr	34	Val	23	Ile	43	100
AKlse2	Tyr	33	Val	22	Ile	41	96
AKlse3[a]	Tyr	34	Val	27	Leu	37	98
AKlse4	His	27	Arg	21	Leu	36	84

[a]Average of the two chains in asymmetric unit.

To understand the structural basis of these decreased thermal stabilities, the crystal structures of AKlse5 and AKlse6 were determined to resolutions of 1.68 and 1.67 Å, respectively. Data collection and refinement statistics are summarized in Table II. We noted that the beta angles in the unit cell parameters were close to 90°. However, processing the data in higher symmetries significantly increased R_{merge}, suggesting that the monoclinic space group was correct. Both AKlse5 and AKlse6 contain two molecules in their asymmetric units and are structurally similar to other AKs with regard to chain folding, the Ap_5A binding, and domain arrangement (Supporting Information Fig. S2).

Several stabilizing structural features were compared between the two LSE-optimized AKthermo variants and AKthermo to identify the molecular mechanism for the unexpected destabilization following LSE optimization (Table III). Among the three structures, AKlse5 contained the fewest ion pairs and hydrogen bonds. This was also true when counting only those interactions that serve to connect distant regions of the polypeptide. AKlse6, which was generated by excluding formally charged residues from LSE-optimizing substitution, contains more ion pairs than AKthermo while the number of those that bridge distant regions are identical in AKlse6 and AKthermo. AKlse6 contained fewer hydrogen bonds than its template, AKthermo, under all conditions, but the decrease in the number of hydrogen bonds was reduced relative to AKlse5.

Structural comparisons also indicated that LSE optimization of AKthermo decreased the apolar buried surface area (Table III). This was surprising because in the experiment for AKmeso, the reduction in LSE increased the buried apolar surface area [Fig. 2(E)]. In addition, the two LSE-optimized AKthermo variants (AKlse5 and AKlse6) contained more apolar atoms than AKthermo

(Table III). The difference in the buried apolar surface area between AKlse5, the most LSE-optimized variant, and AKthermo was 82 Å^2, greater than the largest increase (66 Å^2 between AKlse4 and AKmeso) observed in the AKmeso optimizations. In fact, the buried apolar surface area calculated for AKthermo was larger than that of AKlse4, which displayed the greatest buried apolar surface area of the AKmeso variants (Table III), suggesting highly optimized hydrophobic packing in AKthermo. Thus, the substitutions designed to reduce LSE likely disrupt local and/or global hydrophobic interactions in AKthermo, resulting in relative thermal destabilization.

DISCUSSION

LSE is an empirical descriptor of conformational variability in short protein sequences, calculated from structural information derived from the Protein Data Bank. The relationship between LSE and the thermal stability of proteins has been studied previously. Hwang and coworkers, who originally developed the concept of LSE, observed a linear relationship between average LSE and T_m values in many protein families.[19] In our previous study, we designed AK variants with enhanced stability based on measures of LSE.[18] In this study, we confirmed that LSE optimization can be an effective method for protein thermal stabilization. However, the current study also revealed cases in which LSE optimization resulted in limited or even negative effects on protein thermal stability. Consequently, the results of the current study provide a unique opportunity to examine both effectiveness and the limitations of LSE optimization as a strategy for protein thermal stabilization.

To elucidate the structural basis of thermal stabilization by LSE optimization, we analyzed the crystal structures of four LSE-optimized AKmeso variants and their template, AKmeso. In our previous study, the structure of AKlse1 was determined and compared with that of AKmeso, but no clear structural mechanism was identified that could account for the increased thermal stability of AKlse1.[21] In this study, the crystal structures of three more AKmeso variants (AKlse2, AKlse3, and AKlse4) were determined. Because the LSE values of the four variants were optimized to various extents, this study allowed the examination of correlations between LSE and specific stabilizing structural features instead of simpler one-to-one comparisons.

The most striking result obtained from structural analyses of the AKmeso variants was that the strong inverse correlation between LSE and the apolar buried surface area (R^2 = 0.98), indicating that more apolar surface area becomes buried as LSE is reduced. However, this is likely not due to changes in the number of apolar atoms, which correlates weakly (R^2 = 0.22) with LSE. Substitutions made for the purpose of reducing LSE may increase the apolar buried surface area, which is often considered a measure of the degree of hydrophobic interactions. Thus, enhanced thermal stabilization is ultimately achieved by optimizing the hydrophobic packing of proteins.

The optimization of hydrophobic interactions has been recognized as an important stabilization strategy in a number of thermally stable AKs. Among the three WT AKs, AKthermo contains the highest apolar buried surface area.[22] Structural comparisons of WT AKs also identified a specific AKthermo residue (Met179) that is involved in hydrophobic contacts with conserved residues[22] and was later found to contribute to thermal stabilization when substituted into AKmeso.[21] Experimental evolution of AKmeso for higher thermal stability also generated several stable variants containing mutations (Q16L, T179I, and A193V) that resulted in better hydrophobic packing.[24,37] Interestingly, one of these mutations, A193V, was also generated in the LSE optimization of AKmeso and was included in each of the three LSE-optimized variants (AKlse1, AKlse2, and AKlse3). A recent computational study also showed that AKmeso could be thermally stabilized by repacking its hydrophobic core.[38] Two of the mutations (L3I and L211I) identified in this computational protein design process were also found in the LSE optimization of AKmeso.

In the LSE optimization of AKmeso, the resulting thermal stabilization was effective but limited. Although all four LSE-optimized AKmeso variants yielded higher T_m values than that of their template, AKmeso, the observed increases in T_m were not completely proportional to the decreases in LSE. AKlse4, the most LSE-optimized AKmeso variant, had a significantly lower LSE value than either AKlse1 or AKlse2, but these three AKmeso variants exhibited similar T_m values (Table I). These results indicate a stability limit for LSE-optimized AKmeso variants. It is also puzzling to note that the AKlse4 structure contained the largest number of stabilizing structural features, such as ion pairs, hydrogen bonds, and apolar buried surface area, among the variants (Table III).

To explain the limitation on thermal stabilization observed in the AKmeso variants, we hypothesized that LSE optimization might stabilize local structural elements while simultaneously disrupting other stabilizing noncovalent interactions that connect distant regions of a given polypeptide. When calculating with only such bridging regions, none of the four LSE-optimized AKmeso variants contained more ion pairs or hydrogen bonds than their template, AKmeso (see the values in parentheses in Table III). By designing two AKlse4 mutants (AKlse4m1 and AKlse4m2) and testing their thermal stabilities, we experimentally demonstrated that residue substitutions for reducing LSE at the expense of stabilizing bridging interactions can decrease overall thermal stability. The

two mutants, in which LSE was less optimized than AKlse4 to maintain interactions that connect distant regions, displayed higher T_m values than AKlse4 (Table III), supporting this hypothesis.

The importance of noncovalent interactions that serve to connect distant regions was also recognized in our previous studies of AKs. In structural comparisons of three WT AKs, such interactions were identified most often in AKthermo.[22] Several of these interactions were later found to contribute to overall stability when substituted into AKmeso.[21,23] In the process of generating AKlse1, we encountered a situation in which LSE optimization damaged the noncovalent interactions bridging distant regions. When residues in AKmeso were substituted with those of AKpsychro for the purpose of reducing LSE, an ion pair between residues 23 and 209 connecting the N- and C-terminal regions of AK was broken, and a mutation introduced into AKlse1 for reconstituting the bridging electrostatic interaction resulted in additional stabilization.[21]

It is interesting to note that a stability limit was also recognized in another thermal stabilization trial of AKmeso. In the computational protein design study by Wilson and coworkers,[38] AKmeso variants were stabilized by repacking the hydrophobic core. The variants also displayed an upper thermal limit that could be exceeded only by introducing additional electrostatic interactions. This finding is consistent with the results of our current and previous studies assuming that the thermal stabilization of AKmeso by LSE optimization resulted from the optimization of hydrophobic interactions. In this study, the introduction of three ion pairs into AKlse4, the most LSE-optimized AKmeso variant, increased its thermal stability. Previously, AKlse1 had been stabilized to different extents by adding one to three ion pairs.[21]

While the LSE optimization of AKmeso generated more thermally stable variants, reducing the LSE of AKthermo decreased its thermal stability. The T_m of AKlse5, in which 21 residues were substituted with those of AKmeso, was 9.4°C lower than that of AKthermo despite its considerably lower LSE value (Table I). One could argue that this is not surprising because mesophilic residues were introduced for the stabilization of a thermophilic target. However, in the LSE optimization of AKmeso, the use of a less stable homologous sequence (AKpsychro) for residue substitutions resulted in significant thermal stabilization as evidenced by the three LSE-optimized AKmeso variants (AKlse1, AKlse2, and AKlse3).[18] These three variants contained 10 to 23 substituted residues from AKpsychro yet displayed increases in T_m up to 11.3°C (Table I).

We speculated that the destabilization encountered during the reduction of the LSE of AKthermo to generate AKlse5 was the result of destruction of three ion pairs (Lys19-Glu202, Arg116-Glu198, and Lys180-Asp114) that served to connect distant regions of AKthermo (Fig. 3).[22] To test this hypothesis, we generated another AKthermo variant, AKlse6, by excluding formally charged residues from the substitution pool during LSE optimization. Although the thermal stability of AKlse6 was improved relative to that of AKlse5, its T_m remained lower than that of its template, AKthermo. This suggests that the loss of the ion pairs was not solely responsible for the observed decrease in thermal stability.

Structural analysis revealed that both AKlse5 and AKlse6 contained significantly reduced apolar buried surface areas compared with their template, AKthermo, despite increases in the number of apolar atoms (Table III). This suggests that LSE optimization might disrupt not only stabilizing ion pairs, but also favorable hydrophobic interactions in AKthermo. It seems that AKthermo, like many other natural thermophilic proteins, already possesses highly organized networks of stabilizing structural features such as ion pairs and hydrophobic interactions that are easily damaged by substituting certain residues. Thus, to increase the thermal stability of thermophilic proteins, it is likely necessary to carefully introduce additional stabilizing features while minimizing the destruction of existing ones. This, however, is difficult if detailed structural information is not available for the target proteins.

Despite its limitations, we believe that LSE optimization can still be an effective and efficient method for the thermal stabilization of proteins. As shown in the case of AKlse1, LSE optimization can significantly increase the thermal stability of a mesophilic target (AKmeso) by more than 10°C using only the sequence information from one homologue (AKpsychro). Other stabilization approaches require detailed structural information of the target or a large number of homologous sequences.

LSE optimization may also be useful when combined with other techniques. LSE-optimized sequences can serve as a foundation to which stabilizing mutations identified by other methods are introduced. Alternatively, residues involved in important stabilizing interactions can be excluded from pool of available mutations used in LSE optimization. Previously, the T_m of AKmeso was increased by 26.6°C using LSE optimization simultaneously with other approaches, including structure-guided mutagenesis and molecular evolution.[21] In this study, the thermal stability of AKlse4 was increased by additionally introducing noncovalent interactions identified in structure-based analyses. These results also highlight the importance and complementarity of local conformational stability and global interactions in protein thermal stability.

ACKNOWLEDGMENTS

The authors thank the staff of the beamline 7A of the Pohang Accelerator Laboratory and the GM/CA-CAT

beamline of the Advanced Photon Source for their support with data collection and Christopher M. Bianchetti, Craig A. Bingman, and Jason G. McCoy for their help in the structure determination of AKlse3.

REFERENCES

1. Liszka MJ, Clark ME, Schneider E, Clark DS. Nature versus nurture: developing enzymes that function under extreme conditions. Annu Rev Chem Biomol Eng 2012;3:77-102.
2. Daniel RM, Danson MJ. A new understanding of how temperature affects the catalytic activity of enzymes. Trends Biochem Sci 2010; 35:584-591.
3. Turner P, Mamo G, Karlsson EN. Potential and utilization of thermophiles and thermostable enzymes in biorefining. Microb Cell Fact 2007;6:9.
4. Unsworth LD, van der Oost J, Koutsopoulos S. Hyperthermophilic enzymes—stability, activity and implementation strategies for high temperature applications. FEBS J 2007;274:4044-4056.
5. Eijsink VG, Bjork A, Gaseidnes S, Sirevag R, Synstad B, van den Burg B, Vriend G. Rational engineering of enzyme stability. J Biotechnol 2004;113:105-120.
6. Schoemaker HE, Mink D, Wubbolts MG. Dispelling the myths—biocatalysis in industrial synthesis. Science 2003;299:1694-1697.
7. Vieille C, Zeikus GJ. Hyperthermophilic enzymes: sources, uses, and molecular mechanisms for thermostability. Microbiol Mol Biol Rev 2001;65:1-43.
8. Korkegian A, Black ME, Baker D, Stoddard BL. Computational thermostabilization of an enzyme. Science 2005;308:857-860.
9. Razvi A, Scholtz JM. Lessons in stability from thermophilic proteins. Protein Sci 2006;15:1569-1578.
10. Kiss G, Celebi-Olcum N, Moretti R, Baker D, Houk KN. Computational enzyme design. Angewandte Chemie 2013;52:5700-5725.
11. Socha RD, Tokuriki N. Modulating protein stability - directed evolution strategies for improved protein function. FEBS J 2013;280: 5582-5595.
12. Schmid FX. Lessons about protein stability from in vitro selections. Chembiochem 2011;12:1501-1507.
13. Eijsink VG, Gaseidnes S, Borchert TV, van den Burg B. Directed evolution of enzyme stability. Biomol Eng 2005;22:21-30.
14. Wintrode PL, Arnold FH. Temperature adaptation of enzymes: lessons from laboratory evolution. Adv Protein Chem 2000;55:161-225.
15. Magliery TJ, Lavinder JJ, Sullivan BJ. Protein stability by number: high-throughput and statistical approaches to one of protein science's most difficult problems. Current opinion in chemical biology 2011;15:443-451.
16. Lehmann M, Wyss M. Engineering proteins for thermostability: the use of sequence alignments versus rational design and directed evolution. Curr Opin Biotechnol 2001;12:371-375.
17. Steipe B, Schiller B, Pluckthun A, Steinbacher S. Sequence statistics reliably predict stabilizing mutations in a protein domain. J Mol Biol 1994;240:188-192.
18. Bae E, Bannen RM, Phillips GN Jr. Bioinformatic method for protein thermal stabilization by structural entropy optimization. Proc Natl Acad Sci U S A 2008;105:9594-9597.
19. Chan CH, Liang HK, Hsiao NW, Ko MT, Lyu PC, Hwang JK. Relationship between local structural entropy and protein thermostability. Proteins 2004;57:684-691.
20. Berman HM, Westbrook J, Feng Z, Gilliland G, Bhat TN, Weissig H, Shindyalov IN, Bourne PE. The Protein Data Bank. Nucleic Acids Res 2000;28:235-242.
21. Moon S, Jung DK, Phillips GN Jr., Bae E. An integrated approach for thermal stabilization of a mesophilic adenylate kinase. Proteins 2014; doi: 10.1002/prot.24549.
22. Bae E, Phillips GN Jr. Structures and analysis of highly homologous psychrophilic, mesophilic, and thermophilic adenylate kinases. J Biol Chem 2004;279:28202-28208.
23. Bae E, Phillips GN Jr. Identifying and engineering ion pairs in adenylate kinases. Insights from molecular dynamics simulations of thermophilic and mesophilic homologues. J Biol Chem 2005;280: 30943-30948.
24. Counago R, Chen S, Shamoo Y. In vivo molecular evolution reveals biophysical origins of organismal fitness. Mol Cell 2006;22:441-449.
25. Bannen RM, Suresh V, Phillips GN Jr., Wright SJ, Mitchell JC. Optimal design of thermally stable proteins. Bioinformatics 2008;24: 2339-2343.
26. John DM, Weeks KM. van't Hoff enthalpies without baselines. Protein Sci 2000;9:1416-1419.
27. Otwinowski Z, Minor W. Processing of X-ray diffraction data collected in oscillation mode. Method Enzymol 1997;276:307-326.
28. McCoy AJ, Grosse-Kunstleve RW, Adams PD, Winn MD, Storoni LC, Read RJ. Phaser crystallographic software. J Appl Crystallogr 2007;40:658-674.
29. Vagin A, Teplyakov A. Molecular replacement with MOLREP. Acta Crystallogr Biol Crystallogr 2010;66:22-25.
30. Emsley P, Cowtan K. Coot: model-building tools for molecular graphics. Acta Crystallogr Biol Crystallogr 2004;60:2126-2132.
31. Murshudov GN, Vagin AA, Dodson EJ. Refinement of macromolecular structures by the maximum-likelihood method. Acta Crystallogr Biol Crystallogr 1997;53:240-255.
32. Chen VB, Arendall WB, 3rd, Headd JJ, Keedy DA, Immormino RM, Kapral GJ, Murray LW, Richardson JS, Richardson DC. MolProbity: all-atom structure validation for macromolecular crystallographyActa Crystallogr Biol Crystallogr 2010;66:12-21.
33. Berry MB, Phillips GN Jr. Crystal structures of *Bacillus stearothermophilus* adenylate kinase with bound Ap_5A, Mg^{2+} Ap_5A, and Mn^{2+} Ap_5A reveal an intermediate lid position and six coordinate octahedral geometry for bound Mg^{2+} and Mn^{2+}. Prot Struct Funct Genet 1998;32:275-288.
34. Rodriguez R, Chinea G, Lopez N, Pons T, Vriend G. Homology modeling, model and software evaluation: three related resources. Bioinformatics 1998;14:523-528.
35. Bae E, Phillips GN Jr. Roles of static and dynamic domains in stability and catalysis of adenylate kinase. Proc Natl Acad Sci U S A 2006;103:2132-2137.
36. Glaser P, Presecan E, Delepierre M, Surewicz WK, Mantsch HH, Barzu O, Gilles AM. Zinc, a novel structural element found in the family of bacterial adenylate kinases. Biochemistry 1992;31:3038-3043.
37. Miller C, Davlieva M, Wilson C, White KI, Counago R, Wu G, Myers JC, Wittung-Stafshede P, Shamoo Y. Experimental evolution of adenylate kinase reveals contrasting strategies toward protein thermostability. Biophys J 2010;99:887-896.
38. Howell SC, Inampudi KK, Bean DP, Wilson CJ. Understanding thermal adaptation of enzymes through the multistate rational design and stability prediction of 100 adenylate kinases. Structure 2014;22: 218-229.